Plant Archives

FEASIBILITY OF IRON REMOVAL FROM GROUNDWATER BY USING PUROLITE INC11706 RESIN

Preeti Gahlot[1,2]* Rajesh Dhankhar[1] and Mamta Devi[3,4]

[1]Department of Environmental Science, Maharshi Dayanand University, Rohtak- 124001 (Haryana), India
[2]DPG institute of Technology and Management, Gurgaon, Haryana, India
[3]CSIR National Physical Laboratory, Dr. K.S. Krishnan Marg, New Delhi-110012, India
[4]Academy of Scientific and Innovative Research (AcSIR), Ghaziabad - 201002, Uttar Pradesh, India
*(e-mail: envirojal80@gmail.com; Mobile : 8178060138)

ABSTRACT

Iron (Fe^{2+}) is the major ground water pollutant which demands its efficient elimination. Iron availability in groundwater bespeak assorted geochemical processes along with subsurface contamination in distinct locale. Vulnerability of ground water due to Fe^{2+} contamination cannot be overlooked as this trace metal causes aesthetic issues, health issues and distribution networks deterioration. Although numerous techniques for recovery of iron have been developed and advanced, it was nevertheless not effectively removed. Biosorption technique is stand-alone technique which had the potential for the removal of Iron, and it deploys the mechanism of sorption. The present study aims to investigate the potential of Purolite resins as a low-cost adsorbent for the removal of Fe from ground water. The present study deals with the characterization of Purolite as specific resin adsorbent using SEM and FTIR. The study also investigates the effects of various parameters such as pH, adsorbent dosage, contact time and, initial ion concentration (ionic strength) on the adsorption system. Moreover, adsorption isotherms and kinetics were also evaluated for the process.

***Keywords*:** Iron, resin, adsorption, purolite.

Introduction

Earth crust consists of 5% Iron and all ecosystems include variable amounts of iron, as it is a natural component of the Earth's crust. They cannot be eliminated or degraded, making them stable and persistent environmental pollutants. The impact of human activity altered several metal biogeochemical cycles and balance. The primary human sources of iron are industrial sources, notably industries that produce toothpowder. Furthermore, these are known to have negative and toxic impact seven at low concentrations on the environment and human health (Anusha *et al.*, 2014; Aziz *et al*., 2020).Minerals containing iron can be dissolved by water that seeps through rock and soil. According to Dvorak and Skipton (2007), iron and manganese-containing minerals can percolate through soil and rock and are hence frequently found in groundwater (GW) and some surface waters in significant amounts (Khadse *et al.*, 2015; Baharudin *et al.*, 2015). They are primarily found as ferrous (Fe^{2}) ions in the soluble reduced divalent form. The development of anaerobic conditions in the bottom water zone and the dissolution of iron from floor deposits may be the cause of the presence of dissolved iron in some deep lakes and reservoirs (Abraham *et al.*, 2020). The dissolved species are then dispersed into the overall water body by the annual overturn (Casey, 2009). Finding better and more dependable removal techniques is a constant issue for the water treatment engineer due to the presence of iron in the water (Willey, 1963).

Iron is essential for most forms of life, including humans. Iron can be found in a variety of foods as well as in drinking groundwater. The primary distress about iron in drinking water is its unpalatable metallic aftertaste. Even at a small amount of about 1.8 mg/L, the taste of iron in drinking water can be easily detected (Mane *et al*., 2013). The "BIS (Bureau of Indian Standards) permissible limit for iron in drinking water is 0.3 mg/l"; exceeding this limit in public supplies causes turbidity, inadequate taste and odor, and staining of laundry and plumbing (Elsheikh *et al*., 2020). Therefore, it is crucial to comprehend groundwater quality restoration. The filtering ability of soil has a significant impact on the behavior and transit of pollutants in groundwater because it can change the concentration of minerals and other groundwater constituents (Baharudin *et al.*, 2017).

The decomposition of iron-containing rocks is the most common source of iron in GW. Iron contamination of water is also caused by industrial waste, rusting or corrosion of water supply pipes and reservoirs. Water from wells and springs with immense iron levels may emerge colorless at first, but as the water is exposed to oxygen, brown (iron) orange stains appear. Kidney disease, cancer, anemia, and metabolic disorders can be detected with long-term vulnerability to high levels of Fe^{2+} ions in drinking water (Davison *et al*., 2002). Until now, a great deal of effort has been put into developing techniques for collecting Fe^{2+} ions,

such as oxidation-precipitation-filtration, membrane technology, chemical precipitation coagulation, ion exchange, lime softening, supercritical fluid extraction, aerated granular filters, sub-surface iron removal, bioremediation, and electrolytic reduction (Khatri *et al*., 2017). Iron removal methods that are most commonly used are lime softening, oxidation-precipitation-filtration, membrane processes and ion exchange. The disadvantages of the ion exchange process, such as the resin cost, recovery and its expense, and waste clearance, make the process economically unfeasible. However, it was discovered that these methods have several drawbacks, "if any oxidation occurs during the process, the resulting precipitate can coat and foul the ion exchange media", which is one of the major drawbacks of using this method.

The main aim of present work is to find out the iron removal from groundwater using commercially available resin. The removal examination was done out by differing the effect of adsorbent dose, pH, contact time and initial iron (Fe) concentration.

Materials and Methods

Characterization

SEM is used to characterize the images in order to study the surface and pore morphology, pore size distribution, the porosity and size of the particles for adsorption (Buvaneswari and Singanan, 2020).

FTIR spectroscopy is for obtaining a biochemical fingerprint of the sample under investigation, it is a non-invasive, label-free method and provides details on the quality and structure of the sample's key biomolecules, as well as their chemical modifications (Ami *et al*., 2018). FTIR is most used technique in biosorption process (Michalak *et al*., 2018). FTIR analysed the surface characterization of the adsorbent and showed chemical modifications after adsorption of ions. It was done for analysis of major functional group present in the resins used as sorbent of Iron. FTIR spectra of Iron loaded Purolite resin were obtained to determine adsorption at the stretching and bending sites of active functional groups present in native resins. FTIR peaks on native resin spectra were allocated to different functional groups and bonds in accordance with their Wave numbers (cm^{-1}).

Batch experiments

The adsorption capacity of Purolite resin for Iron removal was determined through batch experiment. The batch experiments were carried out as a function of pH, biosorbent dose, contact time, rpm, the volume of sample, and initial ion concentration of metal ions. All experiments were conducted in triplicate and the average values of each were considered for the future perspective. The batch experiments were conducted in 250 ml conical flasks. Except for the parameter and sample volume, all optimization experiments were carried out in 100 ml of synthetic metal ion solution. For the batch studies, a rotary shaker set to 150 rpm was engaged. Subsequently, the solution was allowed to stand for 10 minutes once attaining equilibrium to allow the absorbents to settle down. After the gravitational settlement of adsorbent, the solution was filtered using Whatman filter paper (No. 1) and the filtrate was thereafter centrifuged for 120 minutes and 30 minutes for Purolite and Chitosan

respectively. Further, the solution was passed for AAS and SPANDS for the detection of Iron and fluoride respectively.

To find the optimum metal ion concentration for adsorption on Purolite, experiment on solution with optimum pH and dose with contact time of 120 min and 60 min respectively were conducted. A range between 5 to 40 g for iron was selected. For the present experiment, varying contact time ranges from 10 to 120 minutes was set with optimum agitation speed as 150 rpm.

Table 1: The Physico-chemical properties of Purolite INC11706 Resin-Iron

S. No.	Parameters	Value
1.	Polymer structure	Macroporous Polystyrene cross-linked with divinylbenzene
2.	Ionic form	Na^+
3.	Particle size range	300-1200 μm
4.	Specific gravity	1.3
5.	Moisture retention	35-40% (40%)
6.	Uniformity coefficient (max.)	1.7

Results and Discussion

Characterization of adsorbent

(i) SEM

Structural and morphological analysis by SEM showed treatment of Iron using Purolite is a complex phenomenon. A considerable modification on the Purolite resin had been observed before and after the iron adsorption (Figure 1). After iron adsorption the size of the nobs got reduced. Before the adsorption the size varied between 228.1 nm to 379.9 nm. However, after adsorption it reduced to 85.3 nm to 182.1 nm. Earlier the surface seemed to be smooth and transparent which after adsorption turned into rough morphology. Nodosites are observable distinctly before adsorption which got packed after adsorption forming lump like structures.
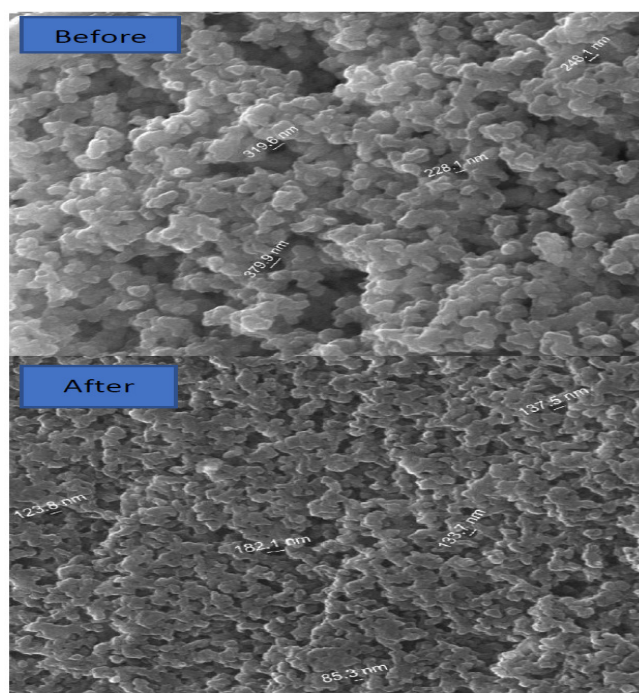

Fig. 1 : SEM micrographs of purolite resin before and after Iron treatment from groundwater

3.1.2. FTIR

It is observed that a non-significant shift is occurring at lower wavelengths with an increasing relative intensity at few bands after the adsorption (Figure 2). There had been significant change in peak ranging from 400 cm^{-1} to 1800 cm^{-1}. This indicates the interaction of iron with nitrogen atom of the tertiary amino group in Purolite. A broad peak is observed at 3600 cm^{-1} which is due to the (O-H) stretching. The presence of free hydroxyl groups and bound O-H bands is indicated by the presence of O-H stretching vibrations that occur over a wide frequency range. After the adsorption process a band of great intensity in 2000 cm^{-1} was observed on the spectra.
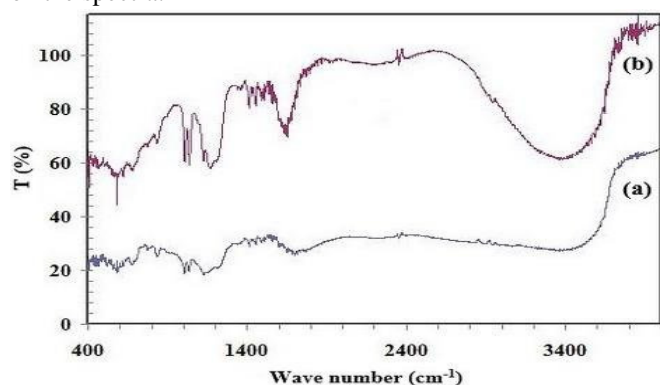

Fig. 2 : FTIR of Purolite resin before and after iron treatment.

Batch Adsorption Experiment

In the experiment:

- Initial Iron (Fe^{2+}) ion Concentration was 5 mg/L

- Adsorbent Dosage was 2g/L
- Contact Time was 30 min., and
- Shaking speed was 150 rpm

3.2.1. Effect of pH on removal of Iron with Purolite resin

The extent of adsorption was analyzed between pH 2-8. From Figure 3, it is clear that the removal of Iron increases as pH increases from 2-7. Once the pH starts increasing after 7, the adsorption cum removal rate starts declining. However, the adsorption of Fe^{2+} was not so significant as observed in case of Chitosan. Only marginal increase in adsorption of Fe^{2+} was observed with the escalation of pH. As with the scale of pH 2 there was effective 90.4% removal of Fe^{2+} which was as enormously highly efficient removal. pH 6 was discovered to be the optimum pH with the removal efficiency of 99.1%. Foreseen, the removal efficiency dwindled from pH 7 to 8 with the removal rate of 99% and 83% respectively.
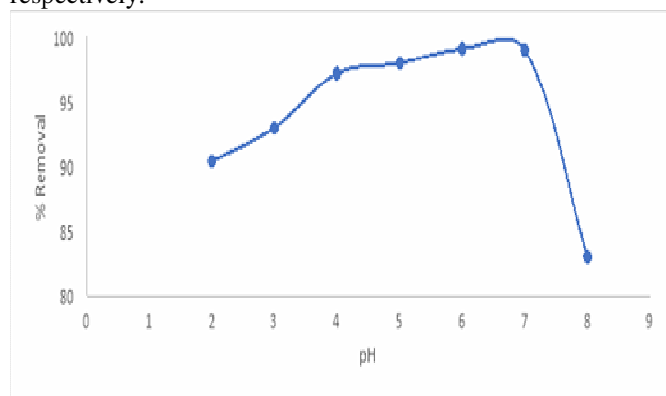

Fig. 3 : Effect of pH on the adsorption of Fe^{2+} on Purolite resin

Coordinate bonds are formed during the ion exchange process that occurs when the adsorption of Fe^{2+} ions occur onto the Purolite. The functional group of purolite is highly dependent on pH as they are very selective for hydrogen ions (Bulai *et al.*, 2011). The sorption occurs with the strong acidic medium (pH=2) and gradually a steady increase has been observed with the decrease in acidity. With the increase in pH the carboxylic functional group become more available for reacting with Iron ions (Bulai *et al.*, 2011).

(ii) Effect of adsorbent dose on removal of iron with Purolite resin

The optimal dosage of adsorbent was discovered to be 0.05 g. At adsorbent dosages of 0.025 to 0.045 g, iron removal rapidly increases, and a steady state is observed until 0.055 g. There were minor variations in terms of elimination, ranging from 0.05 g to 0.055 g. At optimum dose, the percentage elimination was 99.3 percent (Figure 4).
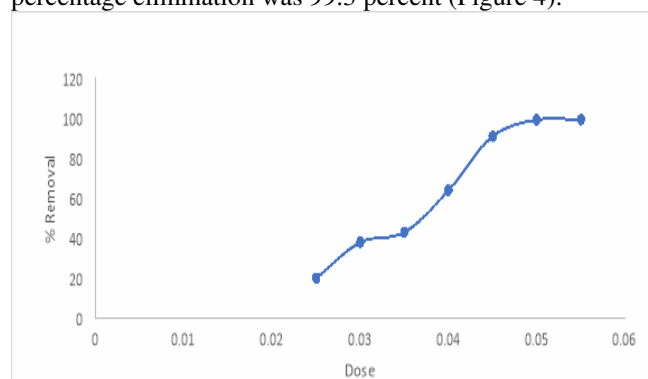

Fig. 4 : Effect of adsorbent dose (g) on the adsorption of Fe^{2+} on Purolite

The availability of a greater number of adsorption sites and a larger surface area resulted in an increase in the rate of adsorption as the adsorbent dose was increased (Gulipalli *et al.*, 2011). However, after certain limit the saturation point is attained, and much removal was not observed which illustrated that the increase in adsorbent doses positively affect the adsorption percentage up till a certain limit.

(iii) Effect of contact time on removal of iron with Purolite resin

Effectiveness of Purolite in removal of Iron was studied under the contact time between 20 to 160 minutes. The effect of contact time in adsorption using Purolite for Iron is shown in Figure 5. The optimum contact time to achieve the state of equilibrium was found to be 100 minutes. Initial uptake started at 20 minutes where the removal efficiency was 43% which turned to 99% as it reached the optimum contact time (100 minutes). Adsorption equilibrium was attained thereafter.
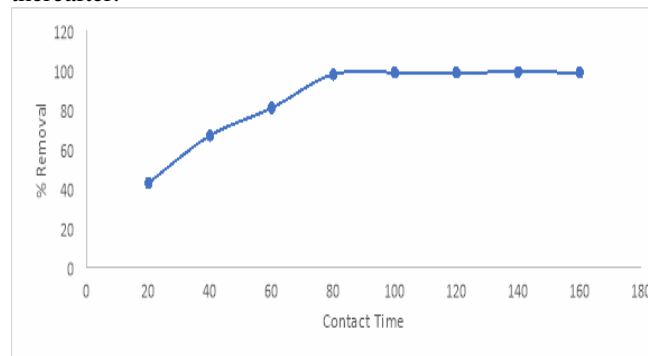

Fig. 5 : Effect of contact time (minutes) on adsorption of Fe^{2+} by purolite

Due to the abundance of adsorption sites, the rate of Iron adsorption binding with Purolite is higher during the initial time of adsorption, and then adsorption slows. This is due to interparticle diffusion, which allows metal ions to enter the adsorbent pores (Gorzin and Abadi, 2018).

(iv) Effect of initial ion concentration on removal of iron with Purolite resin

The influence of iron concentration on its adsorption by Purolite was shown in figure 6. Maximum iron adsorption capacity of Purolite was found to be 97% when the initial iron concentration was 1 g. Once the concentration increases beyond 1 g, the removal efficiency decreases. In Purolite an inverse relationship was observed between the initial iron concentration and its uptake.
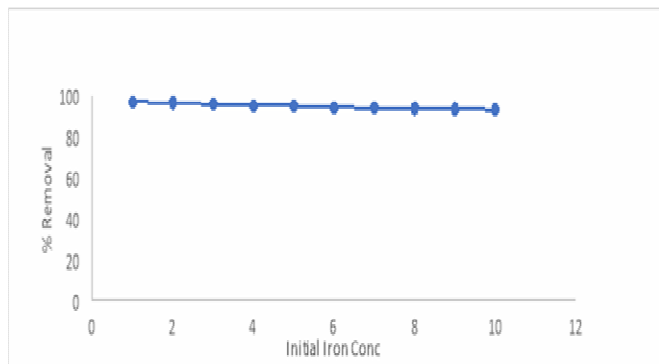

Fig. 6 : Effect of concentration of Fe^{2+} on adsorption process by Purolite

The ratio of initial number of Fe ions to accessible active sites of the adsorbent is low at low initial concentrations; as a result, the removal efficiency of Fe^{2+} is higher, and at higher concentrations, more residual Fe ions remain in the aqueous solution (Gorzin and Abadi, 2017).

3.3. Adsorption Equilibrium isotherm
(i) 3.3.1. Langmuir isotherm

Langmuir isotherm constants (q_{max} and b) were determined for Iron using plots C_e/Q_e versus C_e shown in Figures 7 using Purolite resin. Q_e denotes "the number of ions adsorbed (mg/g) and C_e is the equilibrium concentration of adsorbate (mg/L), b is the Langmuir constant related to energy of adsorption (biosorption intensity) and q_{max} is the maximum sorption capacity". Langmuir constants are represented through Table 4.5. R_L, the separation factor represents the morphology of isotherm and nature of adsorption process as" unfavorable ($R_L > 1$), linear ($R_L = 1$), favorable ($0 < R_L < 1$) and irreversible ($R_L = 0$)".
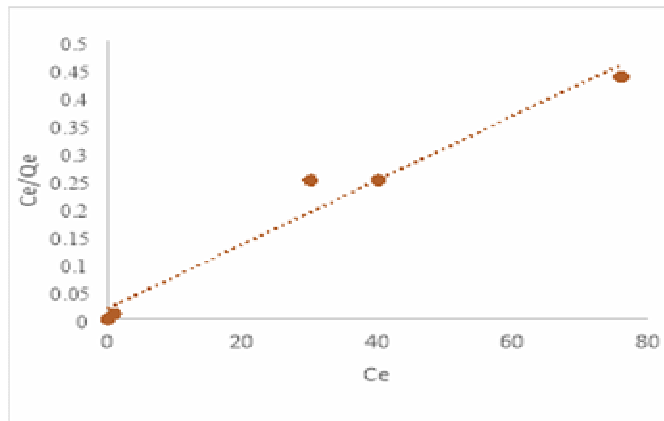

Fig. 7 : Langmuir adsorption curve for Iron adsorption by Purolite

(ii) Freundlich Isotherm

Freundlich isotherm models considers the multilayer coverage and is governed by two constants K_F and n. K_F indicates the adsorption capacity of the adsorbent and n indicates the adsorption intensity (Ngah *et al.*, 2005). The values of Freundlich isotherms constants were determined and were plot as represented in Figure 8.
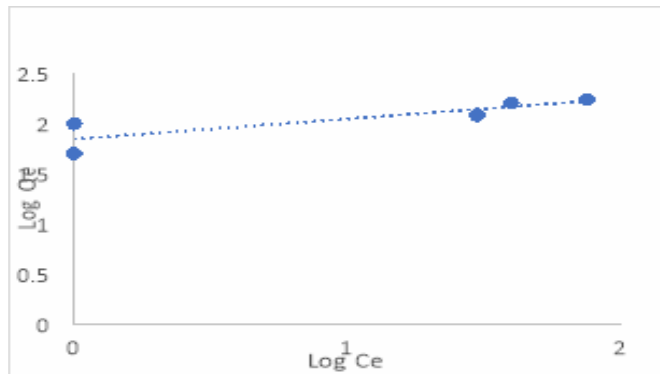

Fig. 8 : Freundlich isotherm curves for Iron adsorption onto Purolite

Higher the value of K_F, lower the adsorption affinity between the ion and the adsorbent. The value of K_F was higher for Purolite for Iron which indicated lower adsorption affinity of Iron onto Purolite. The value of n for Purolite as adsorbent for Iron was between 1-10, which indicated a favorable biosorption (Table 1). The value of correlation coefficient is summarized in Table 2.

Table 1: Langmuir and Freundlich constants for adsorption of Iron on Purolite resin.

Langmuir	
q_m	200
b/K_L	0.263
Freundlich	
1/n	0.202
N	4.95
K_F	69.66

Table 2: Correlation Coefficient (R^2) for Langmuir and Freundlich adsorption isotherms for adsorption of Iron onto Purolite.

Type of Adsorbents	Iron	
	Langmuir	**Freundlich**
Purolite	0.9681	0.7345

Kinetic models

(i) Pseudo First Order

The pseudo first order kinetic was employed to have a better discern of dynamics of adsorption of Iron ions, and for exemplifying the data. Linear plots of the kinetics equation were derived from graphs of log ($q_e - q_t$) against t and t/q_t against t. "q_e and q_t delineate the amounts of metal adsorbed (mg/g) at equilibrium at time t (min)". pseudo first order constants K_1 depicts adsorption rate. The plots of pseudo first order kinetic model obtained for removal of Iron by Purolite (Figure 9).
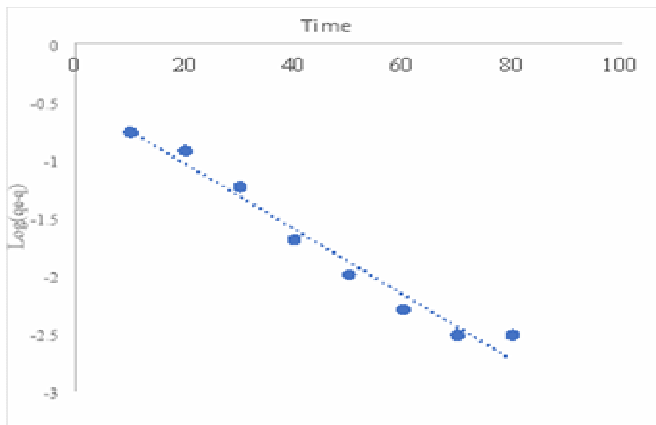
Fig. 9 : Pseudo first order for fluoride adsorption by Purolite resin

The plot shows contrasting changes in log $(q_e - q_t)$ against t for Purolite with respect to adsorption of Iron is shown in Figure 9. The plot showed the values of log $(q_e - q_t)$ decreased with the time of agitation in Purolite. The variation in the rate was not found to be proportional to the first power of concentration for Purolite indicating for Purolite it was not a surface adsorption phenomenon. The value of Lagergren constants is summarized in Table 3.

Table 3 : Lagergren Constants and Correlation coefficients for Iron adsorption onto Purolite

Type of adsorbent	Iron	
	K_1	R^2
Purolite	0.038	0.9829

(ii) Pseudo Second Order

Higher values of correlation coefficients and high proximity of theoretical q_e values educed from plots and calculated experimental q_e values counters the acceptance of pseudo second order equation for Fluoride. The overall process is determined by the amount of adsorbate and accessible sites on the adsorbent's surface with acceptance of second order model. The second-order kinetic model, on the other hand, posits that chemical adsorption is the rate-limiting step (Figure 10). The second-order equation often correlates well with adsorption studies. It's more likely that the adsorption behavior will be influenced by valency forces caused by electron sharing between transition metal cations and the adsorbent (Ngah *et al.*, 2005). The value of constants is summarized in Table 4
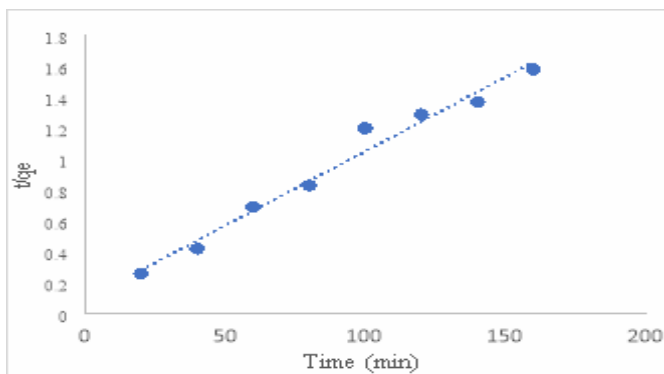

Fig. 10: Pseudo first order for Iron adsorption by Purolite

Table 4: Pseudo Second order constants and Correlation coefficients of Iron adsorption onto Purolite

Type of adsorbent	Iron	
	K_2	R^2
Purolite	0.0010	0.9775

Conclusion

Purolite resin was a favorable ingredient for the elimination of Iron from the aqueous solution and also applicable at domestic level. Adsorption capacity was found to be best at pH 7, which showed that the resin (Purolite SSTC-60) was the best adsorbent applied on the potable water. The optimum time required for removal of Iron was found to be 90 minute from batch experiment. Resin was able to remove as much as 96 % of fluoride at 2g/L of resin dose. Hence, Purolite resin was found to be a viable option for iron removal of water having remarkable concentration of element. The value of qm is 200 which makes it an efficient adsorbent for iron removal.

References

Abraham, N.; James, J.; Banerji, T. and Menon, R. (2020). Development of a novel groundwater iron removal system using adsorptive Fe (II) process. *Groundwater for sustainable development*, 10: 100318.

Anusha, G. and Raja Murugadoss, D.J. (2014). Adsorption of Iron from Aqueous solution using Almond shell as adsorbent. *International Journal of Scientific Research*, 3(10): 1-3.

Aziz, H.A.; Tajarudin, H.A.; Wei, T.H.L. and Alazaiza, M.Y.D. (2020). Iron and manganese removal from groundwater using limestone filter with iron-oxidized bacteria. *International Journal of Environmental Science and Technology*, 17(5): 2667-2680.

Baharudin, F.; Tadza, M.M.; Imran, S.M. and Jani, J. (2018). Removal of iron and manganese in groundwater using natural biosorbent. In IOP conference series: *Earth and Environmental Science*, 140(1) : 012046, IOP Publishing.

Bulai, P. and Cioanca, E.R. (2011). Iron removal from wastewater using chelating resin purolite S930. *TEHNOMUS—new technologies and products in machine manufacturing technologies*.

Buvaneswari, K. and Singanan, M. (2020). Review on scanning electron microscope analysis and adsorption properties of different activated carbon materials. *Materials Today: Proceedings*.

Casey TJ (2009) Iron and manganese in water: Occurrence, drinking water standards, treatment options. Aquavarra Research Publications Water Engineering Papers Aquavarra Research Limited, 22a brook field avenue, Blackrock, County Dublin, Ireland

Davison, A.; Howard, G.; Stevens, M.; Callan, P.; Kirby, R.; Deere, D. and Bartram, J. (2002). *Water safety plans*. WHO/SHE/WSH/02/09 World Health Organization, Geneva, Switzerland.

Dvorak, B.I. and Skipton, S.O. (2007). Drinking water: iron and manganese. Neb Guide published by University of Nebraska-Lincoln Extension, *Institute of Agriculture and Natural Resources*.

Elsheikh, M.A.E.S.; Guirguis, H.S. and Amer, A. (2020). Removal of iron and manganese from groundwater: a study of using potassium permanganate and sedimentation. *MEJ. Mansoura Engineering Journal*, 42(3): 7-12.

Gorzin, F. and Bahri Rasht Abadi, M.M. (2018). Adsorption of Cr (VI) from aqueous solution by adsorbent prepared from paper mill sludge: Kinetics and thermodynamics studies. *Adsorption Science & Technology*, 36(1-2): 149-169.

Gulipalli, C.S.; Prasad, B. and Wasewar, K.L. (2011). Batch study, equilibrium and kinetics of adsorption of selenium using rice husk ash (RHA). *Journal of Engineering Science and Technology*, 6(5): 586-605.

Khadse, G.K.; Patni, P.M. and Labhasetwar, P.K. (2015). Removal of iron and manganese from drinking water supply. *Sustainable Water Resources Management*, 1(2): 157-165.

Khatri, N.; Tyagi, S. and Rawtani, D. (2017). Recent strategies for the removal of iron from water: A review. *Journal of Water Process Engineering*, 19: 291-304.

Mane, P.C.; Kadam, D.D. and Chaudhari, R.D. (2013). Status of some traces metals in water samples from Manjara Dam of Maharashtra, India. *International Journal of Current Microbiology and Applied Sciences*, 2(10): 516-523.

Michalak, I.; Mironiuk, M. and Marycz, K. (2018). A comprehensive analysis of biosorption of metal ions by macroalgae using ICP-OES, SEM-EDX and FTIR techniques. *PLoS One*, 13(10): e0205590.

Ngah, W.W.; Ab Ghani, S. and Kamari, A. (2005). Adsorption behavior of Fe (II) and Fe (III) ions in aqueous solution on chitosan and cross-linked chitosan beads. *Bioresource technology*, 96(4): 443-450.